

# Expansion of Region of Accurate Estimation of Surface Roughness for Application to Carotid Luminal Surface

頸動脈壁内膜面への適用を目指した表面粗さ高精度推定における計測範囲の拡張

Kosuke Kitamura<sup>1‡</sup>, Hideyuki Hasegawa<sup>1,2</sup> and Hiroshi Kanai<sup>2,1</sup> (<sup>1</sup> Grad. School of Biomed. Eng., Tohoku Univ.; <sup>2</sup> Grad. School of Eng., Tohoku Univ.)

北村浩典<sup>1‡</sup>, 長谷川英之<sup>1,2</sup>, 金井 浩<sup>2,1</sup> (<sup>1</sup> 東北大院 医工; <sup>2</sup> 東北大院 工)

## 1. Introduction

Diagnosis of atherosclerosis in an early stage is important to prevent from causing a stroke and heart attack. In early stage of atherosclerosis, the luminal surface of an arterial wall becomes rough as a result of endothelial damage<sup>1</sup>. It would be useful to measure minute surface roughness of the carotid arterial wall for early diagnosis of atherosclerosis. For this purpose, sub-micron resolution is required because endothelial cells are 10-20 μm thick<sup>2</sup>.

Cinthio *at el.* suggested validation of minute roughness measurement using phase tracking<sup>3</sup>. They estimated surface profiles of silicone phantoms, which had ten saw shapes on its surface, during its lateral motion without scanning ultrasonic beams. During a cardiac cycle, the carotid arterial wall moves not only in the radial (= axial) direction but also in the longitudinal (= lateral) direction<sup>4</sup>. This longitudinal movement induces the axial displacement (change in height during longitudinal movement) of the surface at an ultrasonic beam when the surface is rough. This axial displacement could be measured with a sub-micron resolution during the movement of the phantoms of 6 millimeters in the lateral direction. However, the longitudinal displacement of the carotid artery is less than 1 millimeter, and this would limit the length of the region of measurement.

In this study, we proposed a method to increase the measured region using several ultrasonic beams.

## 2. Principle

As shown in **Figs. 1(a)** and **1(b)**, we define the  $k$ -axis and  $r$ -axis in the directions parallel and perpendicular to the arterial wall, respectively. Also,  $k$ -axis and  $r$ -axis in the directions parallel to  $x$ -axis (lateral) and  $z$ -axis (axial), respectively. In addition, the lateral position of the  $m$ -th ultrasonic beam is denoted by  $x_m$ .

During cardiac systole, the vascular diameter is dilated and vascular wall is moved in the longitudinal direction due to an increase of internal pressure at the arrival of the pulse wave (Fig. 1). We can measure the axial displacement  $\Delta d(k(x_m, n), n)$  at the position  $x_m$  of the  $m$ -th ultrasonic beam (including displacement  $\Delta d_g(n)$  caused by global wall motion) and the longitudinal displacement  $\Delta x(n)$  of the arterial wall using block matching<sup>5</sup> for estimation of minute surface profile  $r(k(x_m, n), n)$  using the  $m$ -th ultrasonic beam.

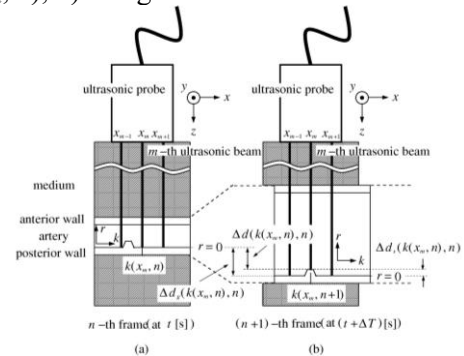


Fig. 1. Illustration of principle of measurement. (a)  $n$ -th frame (at  $t$  [s]). (b)  $(n+1)$ -th frame (at  $(t+\Delta T)$  [s]).

Using phase shift  $\Delta\theta(n)$  of RF signals between  $n$ -th frame and  $(n+1)$ -th frame, the axial displacement  $\Delta d(k(x_m, n), n)$  at the position  $x_m$  of an ultrasonic beam is estimated as:

$$\Delta \hat{d}(k(x_m, n), n) = \frac{c}{2\omega_0} \Delta \hat{\theta}(k(x_m, n), n), \quad (1)$$

where  $c$  is sound speed of the medium (1540 m/s),  $\omega_0 (= 2\pi f_0)$  is the center angular frequency (center frequency  $f_0 = 10$  MHz).

In a region of a few millimeters ( $x$ -axis), axial displacements  $\{\Delta d_g(k(x_{m+i}, n), n)\}$  caused by global wall motion between  $n$ -th frame and  $(n+1)$ -th frame at some positions  $\{x_{m+i}\}$  ( $i = 0, \pm 1, \dots, \pm M$ ) are the same because the wavelength of pulse wave is a few meter, when pulse repetition frequency is 13 kHz. The global displacements  $\Delta d_g(k(x_{m+i}, n), n)$  could be described as:

$$\Delta d_g(k(x_{m+i}, n), n) = \Delta d_g(n), \quad (i = 0, \pm 1, \dots, \pm M) \quad (2)$$

where  $\Delta d_g(n)$  is constant,  $M$  means the number of

E-mail address: kitamura@us.ecei.tohoku.ac.jp  
(kanai, hasegawa)@ecei.tohoku.ac.jp

ultrasonic beams. By assuming that the mean of the axial displacements  $\Delta d_s(k(x_{m+i}, n), n)$  caused by surface roughness is zero, the global displacement  $\Delta \bar{d}_g(n)$  is calculated from the spatial (along  $x$ -axis) mean of the measured axial displacements  $\Delta d(k(x_{m+i}, n), n)$  as:

$$\Delta \bar{d}_g(n) = \frac{1}{2M+1} \sum_{i=m-M}^{m+M} \Delta d(k(x_i, n), n), \quad (3)$$

where  $(2M+1)$  is the number of ultrasonic beams in a region of a few millimeters. By removing this mean displacement  $\Delta \bar{d}_g(n)$  from the original measured axial displacement  $\Delta d(k(x_m, n), n)$ , minute surface profile  $r(k(x_m, n), n)$  is expressed as:

$$\begin{aligned} \hat{r}(k(x_m, n), n) &= r_{m0} + \sum_{n=0}^n \Delta \hat{d}_s(k(x_m, n), n) \\ &= r_{m0} + \sum_{n=0}^n \Delta \hat{d}(k(x_m, n), n) - \Delta \bar{d}_g(n), \end{aligned} \quad (4)$$

where  $r_{m0}$  is initial height  $r(k(x_m, 0), 0)$ , which is defined manually.

**Figure 2** illustrates displacements estimated by the proposed method, where  $\Delta x(n)$  and  $\Delta z(n)$  are estimated by block matching<sup>5)</sup>.

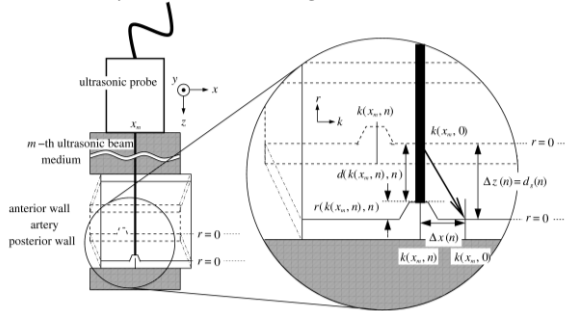


Fig. 2. Illustration of some displacements between 0-th frame and  $n$ -th frame.

Using the estimated lateral displacement  $\Delta \hat{x}(n)$ , the position of a point on the arterial wall, where the  $m$ -th ultrasonic beam crosses at the  $n$ -th frame is defined as  $k(x_m, n)$ . The position of the point in the 0-th frame  $k(x_m + \Delta \hat{x}(n), 0)$  needs to be identified. In this way, as shown in **Fig. 3**, we can express surface profile  $r(k(x_m, n), n)$  of the arterial wall as surface profile  $r(k(x_m + \Delta \hat{x}(n), 0))$  depending on longitudinal ( $x$ -axis) position  $x_m + \Delta \hat{x}(n)$  of the arterial wall at the 0-th frame, where lateral displacement  $\Delta \hat{x}(n)$  is estimated by block matching<sup>5)</sup>.

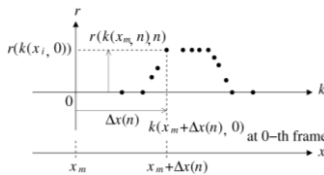


Fig. 3. Illustration of principle to detect the lateral position  $k(x_m + \Delta \hat{x}(n), 0)$ .

Thus far, we considered the estimation of surface roughness using one ultrasonic beam. Moreover, we connect estimated profiles estimated

using adjacent ultrasonic beams by adjusting  $r_{m0}$ .

In a basic experiment, we used two silicone phantoms, which had ten saw teeth shapes on its surface. Also, two phantoms were moved in the axial and lateral (back and forth 1 mm) direction using an automatic stage to simulate arterial wall motion.

### 3. Results

As shown in **Fig. 4**, the average heights of the estimated surface profiles were estimated by proposed method to be  $4.4 \mu\text{m}$  and  $15.0 \mu\text{m}$ , respectively. In contrast, those were measured by a laser profilometer to be  $8 \mu\text{m}$  and  $23 \mu\text{m}$ , respectively. Also, estimated periodicity pitches of saw teeth agreed well with those of obtained by laser profilometer. These results showed that the surface roughness of phantoms could be estimated by the proposed method.

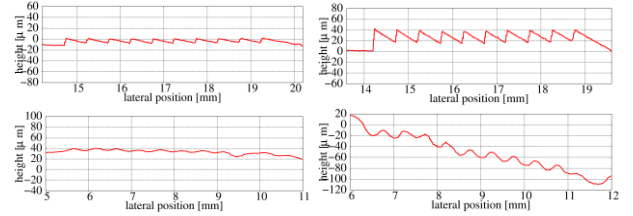


Fig. 4. Estimated surface profiles. Two above figures are heights of shapes obtained by a laser profilometer (average:  $8 \mu\text{m}$  and  $23 \mu\text{m}$ ). Two below figures are those obtained by the proposed method (average:  $4.4 \mu\text{m}$  and  $15 \mu\text{m}$ ).

### 4. Conclusion

In this study, the minute surface roughness of 6 millimeters in length in the lateral direction of the phantoms, which were moving in the axial and lateral (back and forth 1 millimeter) directions, could be measured in the basic experiment. Further investigation will be conducted to measure the surface roughness of the arterial wall *in vivo*.

### References

1. E. Sho, M. Sho, T. M. Singh, H. Nanjo, M. Komatsu, C. Xu, H. Masuda and C. K. Zarins: *Exp. Mol. Pathol.* **73** (2002) 142.
2. Y. Uehara, I. Saito, T. Kushiro and F. Nakamura: *MEDSi, Tokyo* (1995) 16.
3. M. Cinthio, H. Hasegawa and H. Kanai: *IEEE Trans. Ultrason. Ferroelectr. Freq. Control* **58** (2011) 853.
4. M. Cinthio, Å. R. Ahlgren, T. Jansson, A. Eriksson, H. W. Persson and K. Lindström: *IEEE Trans. Ultrason. Ferroelectr. Freq. Control* **52** (2005) 1300.
5. S. Golemati, A. Sassano, M. J. Lever, A. A. Bharath, A. Dhanjil and A. N. Nicolaides: *Ultrasound Med. Biol.* **29** (2003) 387.